Broadband THz Absorber for Large Inclination Angle TE and TM Waves

Vinit Singh Yadav, *Member, IEEE*, Brajesh K. Kaushik, *Senior Member, IEEE*, and Amalendu Patnaik, *Senior Member, IEEE*

***Abstract*—Terahertz (THz) electromagnetic wave absorbers are finding new applications both in military and civilian sectors. This is the reason why constant efforts have been made worldwide to enhance the working performance of these absorbers. One downside of the available absorbers is their response to Transverse Electric (TE) and Transverse Magnetic (TM) waves at different frequency bands. Specific strategic applications require response of an absorber in same frequency band for TE and TM electromagnetic waves, for large inclination and polarization angle of the incoming signal. In this work, we present a metasurface based THz absorber with improved functionality. The fractional bandwidth is 91.64% w.r.t the center frequency of 1.97 THz, that shows an absorptivity of more than 90%. Due to the fourfold symmetry, the absorber is polarization insensitive. It shows more than 80% absorptivity for incoming wave inclinations upto 60°. The thickness of the absorber is $\sim \lambda/11$. The good point is that the absorber shows all these improved performance for both TE and TM incoming signals in the same frequency range. Overall, the designed absorber is a much improved version of its peers available in the literature.**

***Index Terms*—Graphene, metasurface, absorber.**

I. Introduction

BECAUSE of crowding in the low frequency region, higher frequencies are constantly being explored and now the focus is THz region of the spectrum. Although a fully functional THz wireless system is still at its infancy, the priority is to keep all individual THz devices like sources, transmitters, receivers, power splitters, etc., in place. Wave absorber is one such component [1], [2], and at THz frequency, it has some useful applications like imaging, sensing, and cloaking [3], [4]. It is getting its prominence both in civilian and military applications.

There are the different mechanisms of absorption of electromagnetic (EM) wave. In one case the absorption occurs due to the occurrence of Lorentzian electric and magnetic resonance, which leads to the impedance match of the structure to the free space. This in turn power dissipation in the materials. Another type of absorption is because of multi-path reflection that causes complete destructive interference in the reflective component of EM wave [5]. Alternatively, absorption can also occur due to out of phase wave, which are re-radiated waves from induced electric and magnetic currents, nullifying each other in reflection. [6]. Here, in this paper, the impedance matching is used to design a broadband, polarization insensitive THz absorber that can handle large variations of incoming wave inclinations.

Metamaterials, a new type of artificial materials have been investigated in past two decades and have gained a great interest due it's EM properties which are not present in conventional materials. These are the periodic structures with unit cell size of the order of quarter wavelength. The permittivity and permeability of metamaterial are negative, which leads to negative refractive index. This characteristics of these artificial materials make them suitable for applications like polarizer, and absorber [7]–[10]. Landy *et al.* have investigated that for metamaterial absorber (MA), the dimension of unit cell resonator should be such that the surface impedance must be matched to that of free space [11]. Since then, many metasurface devices in the frequency ranging from microwave to terahertz have been proposed to obtain the perfect absorber, wide angle absorber, polarization insensitive absorber, and frequency tunable absorber [12]–[15]. Narrow-band absorbers are not suitable for practical applications [16], [17]. Absorbers based on two ring resonators, lumped elements loading, bi-isotropic, and asymmetrical structures show wide-band behavior [18]–[21]. Frequency reconfigurability in metamaterial based absorbers can be obtained with the addition of provision for change of its geometrical parameters. Multi-layered structures have also been reported in the literature for obtaining frequency tunability in metamaterial based absorbers, but number of layers makes the structure bulky, which is a concern specifically for spacecraft and similar objects [22]–[24].

Graphene is a two-dimensional lattice structure of carbon atoms arranged in a hexagonal form like a honeycomb. Graphene has attracted considerable attention from researchers due to its unique electromagnetic and electric conductive properties [25]. This material has more applications in THz frequency than in the lower region. Narrow-band and dual-band absorbers have been proposed using graphene stacks on amorphous SiO_2 [26], [27]. Multilayer and two layers graphene stacks have been used to get a wide absorption bandwidth. Graphene compounds in organic form were used in RADAR communication to get signal absorption in X-band [28]. Besides the large electrical thickness of some of these graphene based absorbers, one of the key bottlenecks is their response to TE and TM waves at different frequency regions, thereby making it not much useful in strategic applications. In this paper, we have designed a graphene based

Manuscript received July 12, 2021; revised August 26, 2021; accepted September 11, 2021. Date of publication September 14, 2021; date of current version October 4, 2021. This work was supported by the Indian Space Research Organization, India under Grant ISRO/RES/3/760/20-21. *(Corresponding author: Amalendu Patnaik.)*

The authors are with the Department of Electronics and Communication Engineering, Indian Institute of Technology, Roorkee 247667, Uttarakhand, India (e-mail: vinitsingh.iitr@ieee.org; bkk23fec@iitr.ac.in; apatnaik@ieee.org).

Digital Object Identifier 10.1109/JPHOT.2021.3112550

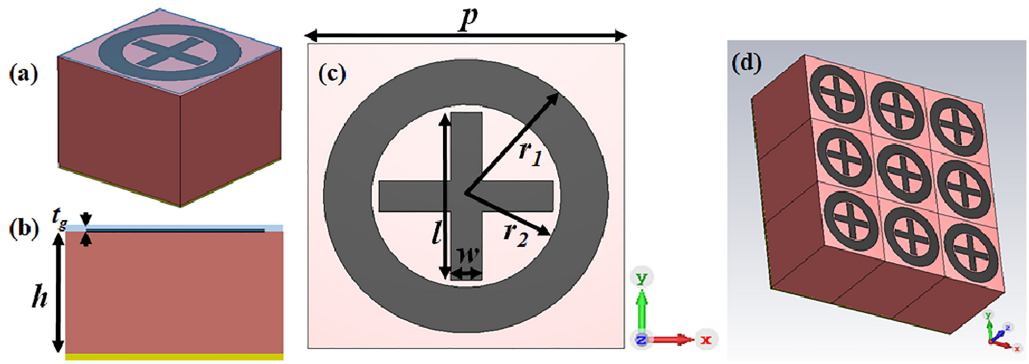

Fig. 1. (a) The metasurface unit cell. (b) Side view of the metasurface unit cell. (c) Top view of the metasurface unit cell and (d) perspective view of metasurface unit cell array operating in Mid-THz frequency regime.

wide-band metasurface absorber for THz frequency regime. The proposed absorber contains mono-layer graphene film on top of a metal-backed dielectric (Amorphous SiO_2). The graphene layer of unit cell is perforated in a plus shape and circular ring form to get two different nearby resonating frequency bands so that they can form a wide-band of absorption in THz frequency regime. The structure is ultra-thin compared to the existing meta-surface absorbers. It provides an ultra wide-band frequency of operation that is not available until now as far as our knowledge goes. The absorptivity of more than 80% has been obtained for different angle of incidence electromagnetic wave up to 60°, for transverse electric (TE) and transverse magnetic (TM) mode of polarization. The structure is polarization insensitive for both TE and TM modes.

II. Absorber Structure and Analysis

The absorber structure consists of periodic array of mono-layer graphene film placed on amorphous silicon dioxide (SiO_2) substrate with dielectric constant 2.2 and loss tangent 0.001 in the operating frequency range. A conducting metallic layer is placed at the backside of dielectric substrate which works as electrode for biasing the graphene layer. The unit cell of the proposed periodic structure is placed along the *x*-*y* plane and the physical dimensions of the unit cell is of sub-wavelength size. The dimensions are optimized to get two nearby absorption frequency bands. The perspective view of the proposed MA is shown in Fig. 1(a). The side view, top view and array of unit cells of proposed metasurface structure are shown in Fig. 1(b), Fig. 1(c), and Fig. 1(d), respectively.The optimized dimensions of the unit cell are $p = 20\ \mu$ m, $h = 25.4\ \mu$m, $r_1 = 9\ \mu$m, $r_2 = 6\ \mu$m, $w = 2\ \mu$m, $l = 11\ \mu$m. The proposed graphene based metasurface absorber has been designed and simulated using CST Microwave Studio version 2021, that is based on finite difference time domain method [29]. 18,482 number of tetrahedral messes have been used to simulate the unit cell of the structure. Two Floquet modes were excited to check the response of the structure for indecent wave.

The thickness of bottom gold layer is 0.5 μm and the conductivity of the thin gold film is considered as 4.56×10^7 S/m in the operating frequency region. The incident electromagnetic wave is seems to be coming from $+z$ direction and the wave is linearly

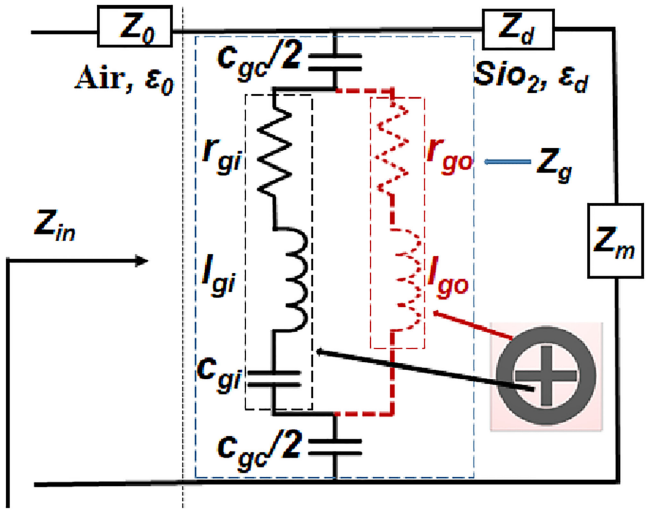

Fig. 2. Equivalent circuit diagram of the proposed MA over a wide-band frequency.

polarized in *x* direction. The absorption *A* in terms of scattering parameters is $A = 1 - S_{11}^2 - S_{21}^2$, where S_{11} is reflection coefficient and S_{21} is transmission coefficient as depicted in Fig. 3 and Fig. 4, respectively. Here the thickness of bottom metal layer is larger than the skin depth so that the incidence EM waves get reflected back in the substrate medium from top of the bottom gold material. Hence the transmission coefficient $S_{21}^2 = 0$.

A. Circuit Equivalent of the Metasurface Absorber

The input impedance of the absorber has to match with the free space impedance in order to have minimum reflection of the incident signal from the absorber. The occurrence of minimum reflection in a broad frequency range is basically due to two separate regions of the unit cell. The one region is the outer ring structure that corresponds to a lower resonance and the second region is the plus shaped structure that corresponds to a higher resonance. In order to explain this concept, a representative circuit diagram is shown in Fig. 2 [30]. In the circuit diagram l_{gi} and r_{gi} are the series inductance and loss resistance of plus shaped graphene based patch. c_{gi} is the capacitance formed between circular ring and plus shaped graphene based patch.

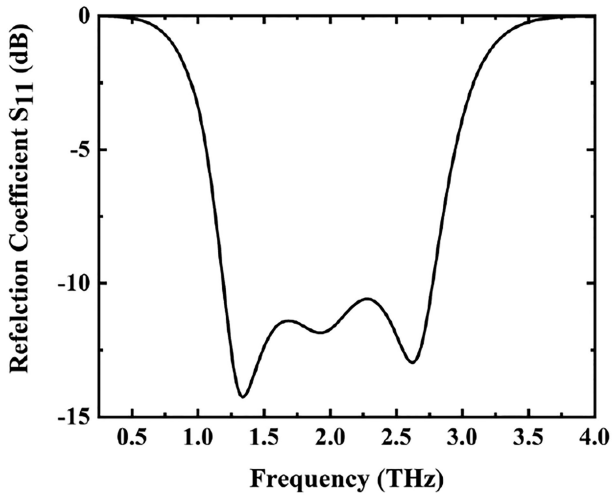

Fig. 3. Reflection coefficient of the proposed graphene based MA over a THz frequency regime.

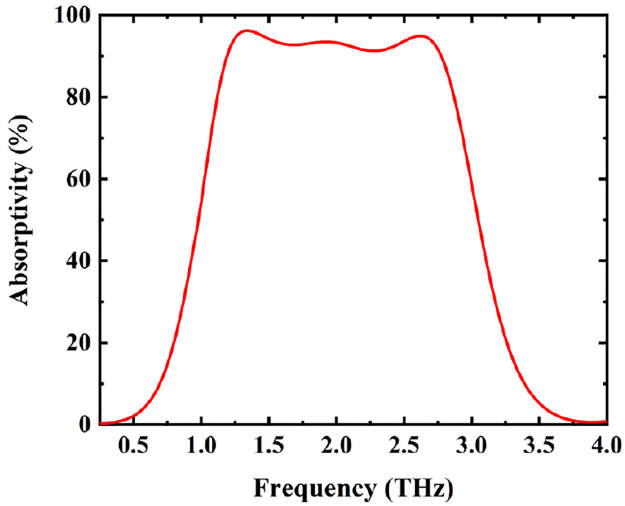

Fig. 4. Absorptivity of the proposed graphene based MA over a THz frequency regime.

l_{go} and r_{go} are the series inductance and loss resistance due the circular patch of graphene and c_{gc} is fringing capacitance. At higher resonant frequency of 2.65 THz, the circuit elements r_{gi}, l_{gi}, c_{gi}, and c_{gc} are effective to calculate the equivalent graphene layer impedance. The circuit elements r_{go}, l_{go} and c_{gc} are responsible to calculate the equivalent surface impedance of graphene layer at lower resonant frequency 1.23 THz and it can be given by

$$Z_g = r_{go} + \left(j\omega l_{go} + \frac{1}{j\omega \left(c_{gc}/4 \right)} \right) \tag{1}$$

To calculate the graphene surface impedance at resonant frequency 2.65 THz, the circuit have an extra series capacitance c_{gi}, which causes the circuit to resonate at higher frequency as depicted from Fig. 2 and given by (2).

$$Z_g = r_{gi} + \left(j\omega l_{gi} + \frac{1}{j\omega \left(\frac{c_{gc} \times c_{gi}}{4c_{gi} + c_{gc}} \right)} \right) \tag{2}$$

Hence the overall input impedance of the absorber can be written as

$$\frac{1}{Z_{in}} = \frac{1}{Z_g} + \frac{1}{Z_d + Z_m} \tag{3}$$

where, Z_d is transmission line impedance due to dielectric layer and Z_m is due to the metallic layer at the bottom of metasurface array.

B. Effective EM Parameter Calculation

The impedance analysis of the MA can also be done with the help of its calculated EM parameters, *viz.* ε_{eff} and μ_{eff} as given in [31]. The normalized impedance is given by

$$Z_n = \sqrt{\frac{\left(\mu_{r(eff)} + i\mu_{i(eff)} \right)}{\left(\epsilon_{r(eff)} + i\epsilon_{i(eff)} \right)}} \tag{4}$$

where,

$$\varepsilon_{eff} = 1 + \frac{\chi_{es}}{d}$$

$$\mu_{eff} = 1 + \frac{\chi_{ms}}{d}$$

$$\chi_{es} = \frac{2j}{k_0} \frac{1 - S_{11}}{S_{11} + 1}$$

$$\chi_{ms} = \frac{2j}{k_0} \frac{S_{11} + 1}{1 - S_{11}} \tag{5}$$

where, d is the distance traveled by incident EM wave within the structure. The Fig. 5(a) and Fig. 5(b) show Real(ε_{eff} and μ_{eff}) and Imaginary(ε_{eff} and μ_{eff}), respectively, calculated using (4) and (5). It can be marked from these figure that the real μ_{eff} is almost following the real ε_{eff} and the imaginary μ_{eff} is following the imaginary ε_{eff}. Hence, the normalized impedance as calculated from (4) is close to unity over the working frequency band.

III. Performance of the EM Wave Absorber

The proposed MA has been designed to absorb the incidence EM wave in THz frequency regime from 1.1 THz to 3 THz and should have the capability of tuning the frequency range with the help of applied chemical potential across the monolayer graphene film.

A. Effect of Incident Angle and Polarization Angle on Absorptivity

In order to check its polarization insensitivity, the absorber was subjected to incident EM wave with different inclination angles in the simulator. Fig. 6(a) and 6(b) shows the TE and TM mode analysis of incident EM wave at different angle of inclination. As seen from Fig. 6(a), the absorption coefficient remains close to unity for inclination angle upto 60°of incident EM wave in TE mode over the operating frequency from 1.07 THz to 2.88 THz. Hence, the performance of the absorber is very

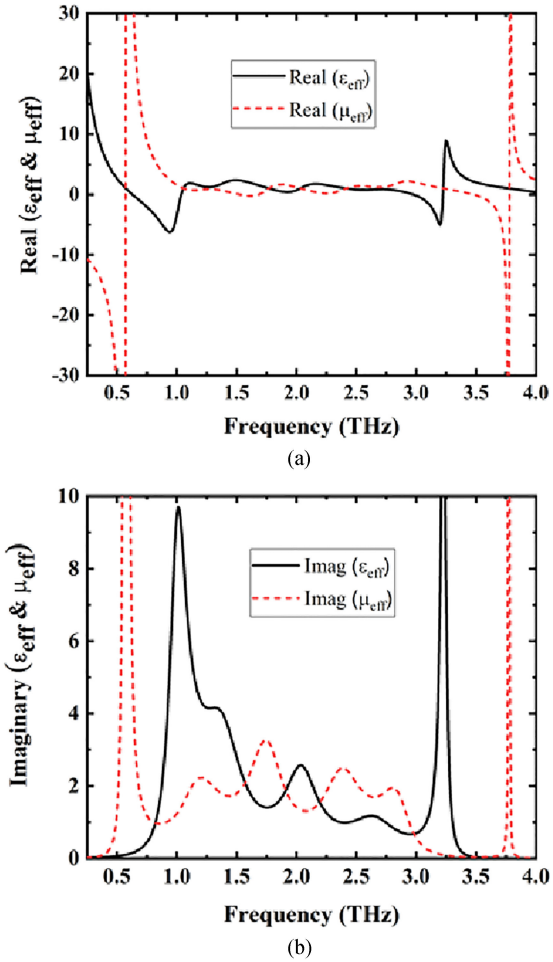

Fig. 5. (a) Real ε_{eff} and μ_{eff}, and (b) Imaginary ε_{eff} and μ_{eff} of the proposed graphene based MA over a THz frequency regime.

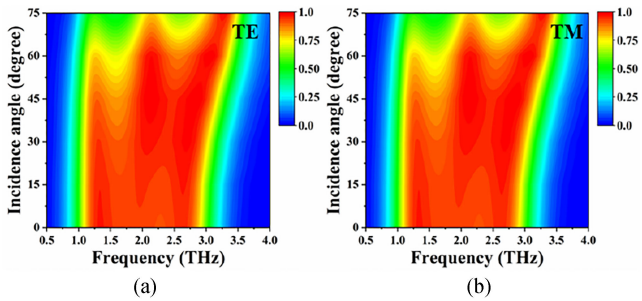

Fig. 6. Absorption coefficient with different incidence angle for (a) TE and (b) TM modes.

good for the incident wave inclination angle in this frequency range. The performance remain same for TM mode also as shown in Fig. 6(b). As far as our understanding goes, this large variation of incident angle has not been reported previously for EM wave absorbers.

The Fig. 7 shows absorptivity of the proposed structure over the operating frequency for different polarization angle. As marked from this figure the absorptivity remains constant for polarization angle from 0° to 45°, making it a polarization insensitive absorber.

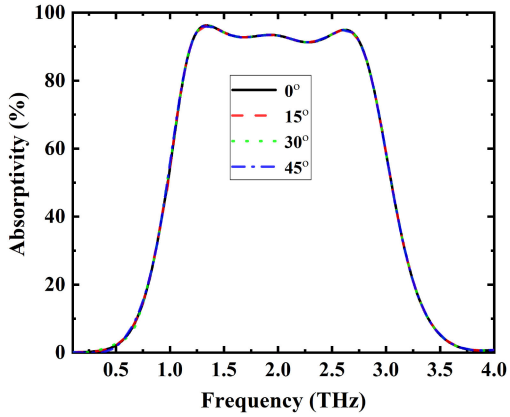

Fig. 7. Absorptivity with frequency over a wide angle of polarization from 0^0 to 45^0.

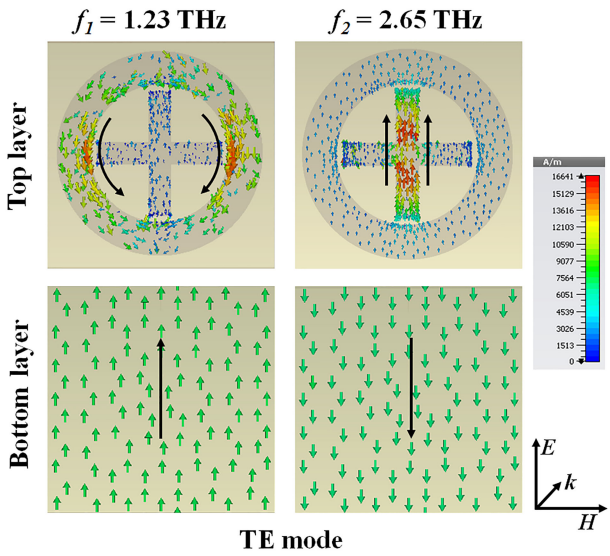

Fig. 8. Surface current distribution of on top and bottom layer of the structure for TE mode.

B. Surface Current and Field Distribution for TE and TM Mode

Fig. 8 shows the surface current distribution for TE mode on top and bottom layer of the unit cell of proposed graphene based MA at resonant frequencies 1.23 THz and 2.65 THz, respectively. For resonant frequency 1.23 THz, the incident EM wave is x-polarized which forms the surface current on the top and bottom layer of the proposed MA. These two top and bottom currents are anti-parallel to each other, and forms an induced magnetic field in y-direction which causes the magnetic resonance [32]. Similarly, for resonant frequency 2.65 THz, the top and bottom surface currents are anti-parallel to each other, and it also forms a magnetic resonance. At resonant frequency 1.23 THz, the effective electrical length of surface current is large due to the circular ring. This causes the lower resonant frequency. Similarly, for resonating frequency of 2.65 THz, the effective electrical length of the surface current is small due to the strip of plus sign of graphene on top of the metal backed dielectric substrate and causes resonance at higher frequency.

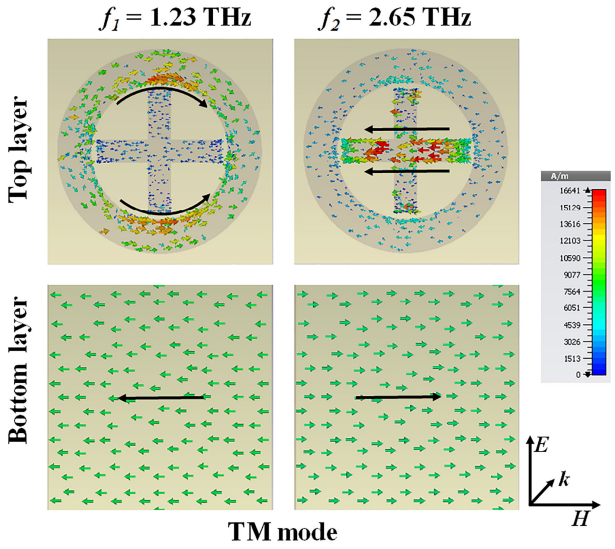

Fig. 9. Surface current distribution on top and bottom layer of the structure for TM mode.

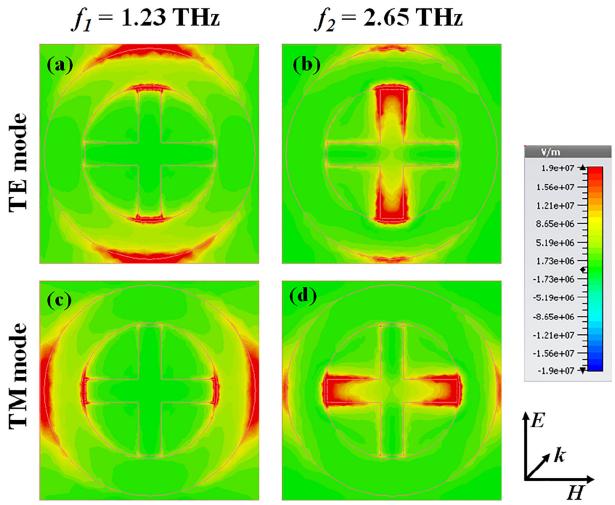

Fig. 10. Electric field distribution on the top surface of proposed graphene based MA at resonant frequencies 1.23 THz and 2.65 THz for TE and TM modes, respectively.

The Fig. 9, shows the surface current distributions for TM mode on top and bottom of the unit cell of proposed graphene based MA. The top and bottom surface current distributions are anti-parallel for both the resonating frequencies at 1.23 THz and 2.65 THz, and forms a perfect magnetic resonance.

The electric field distributions on the top layer of the unit cell of proposed graphene based MA for TE, TM modes are shown in Fig. 10. For TE mode, the Fig. 10(a) and Fig. 10(b) are showing the electric field distribution at resonating frequencies 1.23 THz and 2.65 THz, respectively. For Fig. 10(a), the linearly polarized incident EM wave is x-polarized, and causes resonance at frequency 1.23 THz and which shows the maximum strength of E-field at the corners of circular graphene film. Similarly, for the resonant frequency of 2.65 THz, the E-field distribution is maximum over the vertical strip of plus sign of graphene film on

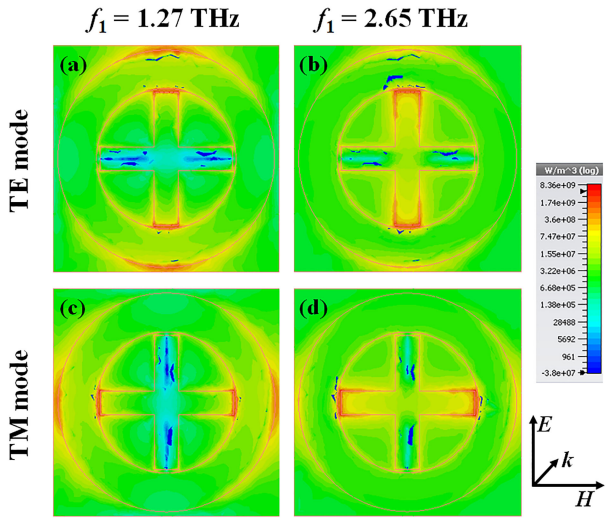

Fig. 11. Power-loss distribution on the top of the proposed MA structure at resonant frequencies 1.23 THz and 2.65 THz for TE and TM mode, respectively.

the unit cell of proposed MA. Similarly, Fig. 10(c) and Fig. 10(d) shows the response for TM mode.

The Fig. 11 shows power-loss density distribution on top of the graphene based MA. In order to ensure maximum surface power loss, the incidence EM wave should be strongly trapped between graphene sheet and bottom metallic layer. The large electric field induce the ohmic loss on the conductive surface (graphene). According to effective medium theory the power loss is mainly due to the thickness of dielectric layer [33], [34]. As observed in Fig. 11, the maximum power loss is distributed in the dielectric. As the transmission coefficient of the structure is zero, the incident EM wave is get absorbed by the structure over a desired frequency range. For TE mode, the power loss density at frequencies 1.23 THz and 2.65 THz are shown in Fig. 11(a) and Fig. 11(b), respectively. Similarly, for TM mode the power loss densities are shown in Fig. 11(c) and Fig. 11(d), respectively.

IV. Fabrication Feasibility and Effect of Graphene Properties on Absorber Performance

Using the well known fabrication techniques, the proposed structure can be assembled and tested. The proposed structure is very thin, and hence for mechanical support, a silicon wafer can be used. The metallic plate as shown in Fig. 1(b), can be grown on a silicon wafer by using e-gun evaporation technique. Further, the spin coated silicon dioxide layer of thickness 25.4 μm, can be formed over yellow metallic layer and has to be exposed to Ultraviolet (UV) rays at 300°C for one hour. Then the graphene can be grown and transferred onto the silicon dioxide layer using chemical vapor deposition technique at atmospheric pressure [35], [36]. As the mono-layer graphene patches are not connected to each other, so for ease of biasing an ion gel can be deposited on top of the graphene layer [37].

Graphene surface conductivity is anisotropic in nature. The Dyadic Green's function for the tensor surface conductivity boundary condition is given in [38]. The two dimensional

graphene sheet is defined as an impedance boundary in the EM simulator, whose surface conductivity is given by the generalized Kubo's formula [39] (although mentioned widely in the literature, for completeness we are here reproducing it again).

$$\sigma(\omega, E_f, \Gamma, T) = \sigma_{inter} + \sigma_{intra} \tag{6}$$

$$\sigma_{intra} = \frac{2k_bTe^2}{\pi\hbar} ln\left(2cosh\frac{E_f}{2k_bT}\right)\frac{i}{(\omega + i\Gamma)} = \frac{\alpha}{-i\omega + \Gamma} \tag{7}$$

$$\sigma_{inter} = \frac{e^2}{4\hbar}\left[H\left(\frac{\omega}{2}\right) + i\frac{4\omega}{\pi}\int_0^\infty \frac{H(\Omega) - H\left(\frac{\omega}{2}\right)}{\omega^2 - 4\Omega^2} d(\Omega)\right] \tag{8}$$

where

$$H(\Omega) = sinh\left(\frac{\hbar\Omega}{k_bT}\right) \Big/ \left[cosh\frac{\hbar\Omega}{k_bT} + cosh\left(\frac{E_f}{k_bT}\right)\right]$$

e is the electron charge, ω is the angular frequency of incident EM wave, $T = 300\,K$ is the temperature, $\Gamma = \tau^{-1}$ is the scattering rate and τ is electron scattering time constant, and can be varied from 0.02 to 2 ps; $\hbar$ is the reduced Planck's constant, and k_b is the Boltzmann constant. If Fermi energy of the graphene conduction band is greater than half of the photon energy, the intraband conductivity dominates over interband conductivity of graphene due to Pauli blocking [40]. The Fermi energy E_f of graphene film can be altered by external applied voltage V_g to the structure. The Fermi energy can be given by

$$E_f = \hbar v_f \sqrt{\frac{\pi\varepsilon_d\varepsilon_0 V_g}{et_2}} \tag{9}$$

where $v_f = 10^6$m/s is the Fermi velocity, V_g is the applied chemical potential to the graphene (here we have considered $V_g = 0.8\,eV$), ε_d is dielectric constant of substrate. In the THz frequency regime the surface conductivity of mono-layer graphene can be given by Drude's conductivity formula:

$$\sigma_g(\omega) = \frac{e^2E_f}{\pi\hbar}\frac{i}{(\omega + i\tau^{-1})} \tag{10}$$

The relative permittivity of graphene in terms of surface conductivity which is also a function of frequency can be given as

$$\varepsilon(\omega) = 1 + i\frac{\sigma_g(\omega)}{t_g\varepsilon_0\omega} \tag{11}$$

The mono-layer graphene thickness can be anything in 0.4 nm – 1.7 nm range [41]. In our case we considered $t_g = 0.65$nm for optimum performance of the absorber. As seen from (7), the surface conductivity of two dimensional mono-layer graphene is a function of angular frequency ω, temperature T, electron scattering constant τ, and applied chemical potential E_f.

Fig. 12(a), shows the variation of absorptivity with the scattering time τ. The scattering time is defined as the interval between successive electron collision time. The increase in scattering time in turn increases the surface conductivity of graphene patch [42]–[44]. It can be seen from Fig. 12(a) that absorptivity is more than 90% over the frequency band 1.07 THz - 2.88 THz for 0.2 ps scattering time constant. Fig. 12(b) shows the effect of change in applied chemical potential across the structure on absorptivity. Altering the applied Fermi energy leads to change in surface conductivity of graphene which in turn leads to variation in resonance frequency of the structure over a wide frequency range as seen from (10) and can be observed in Fig. 12(b). The characteristics of the proposed metasurface based EM wave absorber is compared with that of its counterparts in Table I. The improved performance of our structure can be clearly marked from this table.

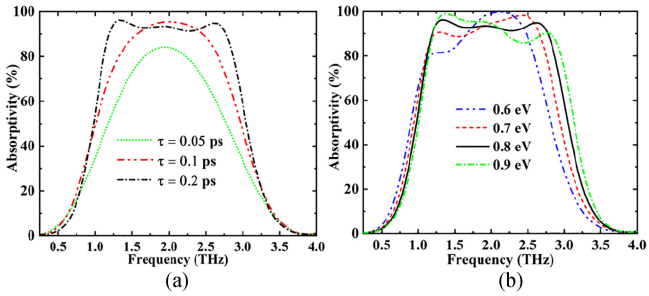

Fig. 12. Absorptivity with frequency by changing the (a) Scattering time constant and (b) Applied chemical potential of the mono-layer graphene film of the proposed MA structure over the THz frequency regime.

TABLE I
COMPARISON OF PROPOSED GRAPHENE BASED MA WITH THE OTHER GRAPHENE BASED ABSORBERS

THz graphene based MAs	Fractional bandwidth	Operating frequency	Dielectric substrate thickness	Period of unit cell
Liu et. al. [45]	37.80%	7-10.2 THz	∼λ/8	∼λ/14
Huang et al. [46]	13.37%	80-95 THz	∼λ/14	∼3λ/4
He et. al. [23]	60%	2-4 THz	∼λ/24	∼λ/14
Fu et. al. [22]	28.26%	5.5-9.5 THz	∼λ/5	∼λ/11
Zhang et. al. [26]	40%, 8%	4.28 THz, 7.50 THz	∼λ/8	∼λ/13
Huang et. al. [30]	70.5%	1.34-2.8 THz	∼λ/200	∼λ/22
Ghosh et. al. [9]	90.34%	3.69-9.77 THz	∼λ/11	∼λ/13
Chen et. al. [27]	7.80%, 3.80%	3.80 THz, 7.36 THz	NA	NA
In this report	91.64%	1.07-2.88 THz	∼λ/11	∼λ/14

V. CONCLUSION

In this paper, a graphene based metasurface absorber is proposed for THz frequency band. A wide-band of absorption is obtained compared to the other available multilayer and single layer graphene based metasurface absorbers. Simulation results reveal similar performance of the absorber for the both TE and TM mode of incoming signal in the entire band of operation. Improved performance of the absorber in terms of fractional bandwidth, thinness of the structure, angle of polarization and inclination of the incoming wave, is obtained. The designed wave absorber is anticipated to add significant value in the ongoing THz devices and application research.

REFERENCES

[1] H. T. Chen, W. J. Padilla, J. M. Zide, A. C. Gossard, A. J. Taylor, and R. D. Averitt, "Active terahertz metamaterial devices," *Nature*, vol. 444, pp. 597–600, 2006.

[2] H. T. Chen *et al.*, "Experimental demonstration of frequency-agile terahertz metamaterials," *Nature Photon.*, vol. 2, pp. 295–298, 2008.

[3] A. Forouzmand and H. Mosallaei, "Real-time controllable and multifunctional metasurfaces utilizing indium tin oxide materials: A phased array perspective," *IEEE Trans. Nanotechnol.*, vol. 16, no. 2, pp. 296–306, Mar. 2017.

[4] S. Khosravi, A. Rostami, M. Dolatyari, and G. Rostami, "Broadband carpet cloak designed using nanocomposite metamaterials for 3 to 5 micrometer wavelength range," *IEEE Trans. Nanotechnol.*, vol. 16, no. 1, pp. 44–48, Jan. 2017.

[5] H.-T. Chen, "Interference theory of metamaterial perfect absorbers," *Opt. Exp.*, vol. 20, pp. 7165–7172, 2012.

[6] H. T. Chen *et al.*, "Experimental demonstration of frequency-agile terahertz metamaterials," *Nature Photonics Photon.*, vol. 2, pp. 295–298, 2008.

[7] V. S. Yadav, S. K. Ghosh, S. Bhattacharyya, and S. Das, "Graphene-based metasurface for a tunable broadband terahertz cross-polarization converter over a wide angle of incidence," *Appl. Opt.*, vol. 57, no. 29, pp. 8720–8726, Oct. 2018.

[8] V. S. Yadav, S. K. Ghosh, S. Das, and S. Bhattacharyya, "Wideband tunable mid-infrared cross-polarisation converter using monolayered graphene-based metasurface over a wide angle of incidence," *IET Microw., Antennas Propag.*, vol. 13, no. 5, pp. 82–87, Jan. 2019.

[9] S. K. Ghosh, V. S. Yadav, S. Das, and S. Bhattacharyya, "Tunable graphene-based metasurface for polarization-independent broadband absorption in lower mid-infrared (MIR) range," *IEEE Trans. Electromagn. Compat.*, vol. 62, no. 2, pp. 346–354, Apr. 2020.

[10] Y. Wang, Q. Wu, Y. M. Wu, K. Zhang, L. W. Li, and J. H. Yin, "Broadband terahertz left-hand material with negative permeability for magnetic response," *IEEE Trans. Magn.*, vol. 47, no. 10, pp. 2592–2595, Oct. 2011.

[11] N. I. Landy, S. Sajuyigbe, J. J. Mock, D. R. Smith, and W. J. Padilla, "Perfect metamaterial absorber," *Phys. Rev. Lett.*, vol. 100, May 2008, Art. no. 207402.

[12] X. Jia, X. Wang, C. Yuan, Q. Meng, and Z. Zhou, "Novel dynamic tuning of broadband visible metamaterial perfect absorber using graphene," *J. Appl. Phys.*, vol. 120, no. 3, 2016, Art. no. 033101.

[13] Y. Bai, L. Zhao, D. Ju, Y. Jiang, and L. Liu, "Wide-angle, polarization-independent and dual-band infrared perfect absorber based on l-shaped metamaterial," *Opt. Exp.*, vol. 23, no. 7, pp. 8670–8680, Apr. 2015.

[14] D. L. Vu *et al.*, "The electromagnetic response of different metamaterial structures," *Adv. Natural Sci.: Nanoscience Nanotechnol.*, vol. 1, no. 4, Feb. 2011, Art. no. 045016.

[15] N. Mattiucci, R. Trimm, G. D'Aguanno, N. Akozbek, and M. J. Bloemer, "Tunable, narrow-band, all-metallic microwave absorber," *Appl. Phys. Lett.*, vol. 101, no. 14, 2012, Art. no. 141115.

[16] Z. Su, J. Yin, and X. Zhao, "Terahertz dual-band metamaterial absorber based on graphene/MgF_2 multilayer structures," *Opt. Exp.*, vol. 23, no. 2, pp. 1679–1690, Jan. 2015.

[17] Y.-P. Zhang *et al.*, "Graphene-based tunable polarization insensitive dual-band metamaterial absorber at mid-infrared frequencies," *Chin. Phys. Lett.*, vol. 32, no. 6, Jun. 2015, Art. no. 068101.

[18] Y. Z. Cheng, Y. Wang, Y. Nie, R. Z. Gong, X. Xiong, and X. Wang, "Design, fabrication and measurement of a broadband polarization-insensitive metamaterial absorber based on lumped elements," *J. Appl. Phys.*, vol. 111, no. 4, 2012, Art. no. 044902.

[19] H. Li, L. H. Yuan, B. Zhou, X. P. Shen, Q. Cheng, and T. J. Cui, "Ultrathin multiband gigahertz metamaterial absorbers," *J. Appl. Phys.*, vol. 110, no. 1, 2011, Art. no. 014909.

[20] O. Ouchetto, B. Essakhi, S. Jai-Andaloussi, and S. Zaamoun, "Homogenization of bi-isotropic multilayered metamaterial structures," *IEEE Trans. Nanotechnol.*, vol. 16, no. 6, pp. 946–953, Nov. 2017.

[21] X. Ling, Z. Xiao, X. Zheng, J. Tang, and K. Xu, "A three-dimensional ultra-broadband metamaterial absorber in terahertz region," *Appl. Phys. A*, vol. 122, no. 11, pp. 1432–0630, 2016.

[22] P. Fu, F. Liu, G. J. Ren, F. Su, D. Li, and J. Q. Yao, "A broadband metamaterial absorber based on multi-layer graphene in the terahertz region," *Opt. Commun.*, vol. 417, pp. 62–66, 2018.

[23] S. He and T. Chen, "Broadband THz absorbers with graphene-based anisotropic metamaterial films," *IEEE Trans. THz Sci. Technol.*, vol. 3, no. 6, pp. 757–763, Nov. 2013.

[24] X. Liu, L. Peng, J. Ma, B. Shi, X. Jiang, and S. Li, "Quasi-two-dimensional hyperbolic metamaterial for mid-infrared wave multiple collimations," *IEEE Trans. Nanotechnol.*, vol. 18, pp. 542–552, 2019.

[25] S. Das *et al.*, "Amplifying charge-transfer characteristics of graphene for triiodide reduction in dye-sensitized solar cells," *Adv. Funct. Mater.*, vol. 21, no. 19, pp. 3729–3736, 2011.

[26] J. Zhang, J. Tian, and L. Li, "A dual-band tunable metamaterial near-unity absorber composed of periodic cross and disk graphene arrays," *IEEE Photon. J.*, vol. 10, no. 2, 2018, Art. no. 4800512.

[27] Y. Chen, X. Pan, Z. Bao, Y. Wang, Z.-D. Hu, and J. Wang, "Tunable terahertz perfect-absorbers with dual peak based on reverse graphene patch metamaterials," *IEEE Photon. J.*, vol. 13, no. 3, Jun. 2021, Art. no. 4800312.

[28] R. Bhattacharyya *et al.*, "Graphene oxide-ferrite hybrid framework as enhanced broadband absorption in gigahertz frequencies," *Sci. Rep.*, vol. 9, no. 1, 2019, Art. no. 12111.

[29] CST Studio SuiteUser's Manual, *Comput. Simul. Technol.*, Darmstadt, Germany, 2016.

[30] X. Huang, X. Zhang, Z. Hu, M. Aqeeli, and A. Alburaikan, "Design of broadband and tunable terahertz absorbers based on graphene metasurface: Equivalent circuit model approach," *IET Microw., Antennas Propag.*, vol. 9, no. 4, pp. 307–312, 2015.

[31] C. L. Holloway, E. F. Kuester, and A. Dienstfrey, "Characterizing metasurfaces/metafilms: The connection between surface susceptibilities and effective material properties," *IEEE Antennas Wireless Propag. Lett.*, vol. 10, pp. 1507–1511, 2011.

[32] Z. L. Mei, X. M. Ma, C. Lu, and Y. D. Zhao, "High-efficiency and wide-bandwidth linear polarization converter based on double u-shaped metasurface," *AIP Adv.*, vol. 7, no. 12, 2017, Art. no. 125323.

[33] G. Duan *et al.*, "A survey of theoretical models for terahertz electromagnetic metamaterial absorbers," *Sensors Actuators A: Phys.*, vol. 287, pp. 21–28, 2019.

[34] N. I. Landy, S. Sajuyigbe, J. J. Mock, D. R. Smith, and W. J. Padilla, "Perfect metamaterial absorber," *Phys. Rev. Lett.*, vol. 100, May 2008, Art. no. 207402. [Online]. Available: https://link.aps.org/doi/10.1103/PhysRevLett.100.207402

[35] J. Pang *et al.*, "Self-terminating confinement approach for large-area uniform monolayer graphene directly over Si/SiOx by chemical vapor deposition," *ACS Nano*, vol. 11, no. 2, pp. 1946–1956, 2017.

[36] Y. Zhang, L. Zhang, and C. Zhou, "Review of chemical vapor deposition of graphene and related applications," *Accounts Chem. Res.*, vol. 46, no. 10, pp. 2329–2339, 2013.

[37] J. T. Kim, H. Choi, Y. Choi, and J. H. Cho, "Ion-gel-gated graphene optical modulator with hysteretic behavior," *ACS Appl. Mater. Interfaces*, vol. 10, pp. 1836–1845, 2018.

[38] S. Hayati Raad, Z. Atlasbaf, M. Shahabadi, and J. Rashed-Mohassel, "Dyadic greens function for the tensor surface conductivity boundary condition," *IEEE Trans. Magn.*, vol. 55, no. 11, pp. 1–7, Nov. 2019, Art. no. 2801807.

[39] W. G. Hanson, "Dyadic green's functions and guided surface waves for a surface conductivity model of graphene," *J. Appl. Phys.*, vol. 103, no. 6, 2008, Art. no. 064302.

[40] L. M. Malard, K. F. Mak, A. H. C. Neto, N. M. R. Peres, and T. F. Heinz, "Observation of intra- and inter-band transitions in the transient optical response of graphene," *New J. Phys.*, vol. 15, no. 1, Jan. 2013, Art. no. 015009.

[41] C. J. Shearer, A. D. Slattery, A. J. Stapleton, J. G. Shapter, and C. T. Gibson, "Accurate thickness measurement of graphene," *Nanotechnol.*, vol. 27, no. 12, Feb. 2016, Art. no. 125704.

[42] P. Neugebauer, M. Orlita, C. Faugeras, A.-L. Barra, and M. Potemski, "How perfect can graphene be?," *Phys. Rev. Lett.*, vol. 103, Sep. 2009, Art. no. 136403.

[43] I. Maeng, S. Lim, S. J. Chae, Y. H. Lee, H. Choi, and J.-H. Son, "Gate-controlled nonlinear conductivity of dirac fermion in graphene field-effect transistors measured by terahertz time-domain spectroscopy," *Nano Lett.*, vol. 12, no. 2, pp. 551–555, 2012.

[44] Q. Zheng and J. Kim, *Graphene for Transparent Conductors*. Hong Kong, China: Springer, 2015.

[45] C. Liu, L. Qi, and X. Zhang, "Broadband graphene-based metamaterial absorbers," *AIP Adv.*, vol. 8, no. 1, 2018, Art. no. 015301.

[46] H. Huang, H. Xia, W. Xie, Z. Guo, H. Li, and D. Xie, "Design of broadband graphene-metamaterial absorbers for permittivity sensing at mid-infrared regions," *Sci. Rep.*, vol. 8, no. 1, pp. 1–10, 2018.